LA-UR- 04-4072

Approved for public release; distribution is unlimited.

Title: CHEMEOS: A New Chemical-Picture-Based Model for Plasma Equation-of-State Calculations

Author(s): Peter Hakel
David P. Kilcrease

Submitted to: Proceedings from The 14th APS Topical Conference on Atomic Processes in Plasmas, Santa Fe, New Mexico, April 19-22, 2004

CHEMEOS:
A New Chemical-Picture-Based Model for Plasma Equation-of-State Calculations

Peter Hakel and David P. Kilcrease

Theoretical Division
Atomic and Optical Theory Group (T-4)
Los Alamos National Laboratory
Los Alamos, NM 87545, USA

Abstract.
We present the results of a new plasma equation-of-state (EOS) model currently under development at the Atomic and Optical Theory Group (T-4) in Los Alamos. This model is based on the chemical picture of the plasma and uses the free-energy-minimization technique and the occupation-probability formalism. The model is constructed as a combination of ideal and non-ideal contributions to the total Helmholtz free energy of the plasma including the effects of plasma microfields, strong coupling, and the hard-sphere description of the finite sizes of atomic species with bound electrons [1, 2]. These types of models have been recognized as a convenient and computationally inexpensive tool for modeling of local-thermal-equilibrium (LTE) plasmas for a broad range of temperatures and densities [3]. We calculate the thermodynamic characteristics of the plasma (such as pressure and internal energy), and populations and occupation probabilities of atomic bound states. In addition to a smooth truncation of partition functions necessary for extracting ion populations from the system of Saha-type equations, the occupation probabilities can also be used for the merging of Rydberg line series into their associated bound-free edges [4].

In the low-density, high-temperature regimes the plasma effects are adequately described by the Debye-Hückel model and its corresponding contribution to the total Helmholtz free energy of the plasma. In strongly-coupled plasmas, however, the Debye-Hückel approximation is no longer appropriate. In order to extend the validity of our EOS model to strongly-coupled plasmas while maintaining the analytic nature of our model, we adopt fits to the plasma free energy based on hypernetted-chain and Monte Carlo simulations [5, 6, 7]. Our results for hydrogen are compared to other theoretical models. Hydrogen has been selected as a test-case on which improvements in EOS physics are benchmarked before analogous upgrades are included for any element in the EOS part of the new Los Alamos opacity code ATOMIC.

INTRODUCTION

In this paper we describe the equation-of-state model adopted for the new Los Alamos low-to-medium-Z opacity code ATOMIC. This EOS model provides LTE ion stage populations calculated with a thermodynamically consistent account of non-ideal plasma effects such as continuum lowering. To this end we have followed a free-energy-minimization approach [3, 8] in deriving the ion population equations for the thermodynamic equilibrium EOS for ATOMIC. The resulting equations can be formulated to resemble modified Saha-type equations with guaranteed thermodynamic consistency since all population and thermodynamic quantities are derived from a single expression for the total Helmholtz free energy $F(V,T,\{N_s\})$ for the entire system. The solution of the system of Saha-type equations is the collection of populations $\{N_s\}_{min}$ which minimizes the free energy at a given temperature and mass density. The formal procedure also satisfies the stoichiometric constraints for ionization or molecular dissociation, as well as overall plasma charge neutrality and mass conservation conditions.

Inherent in this formalism is the use of the chemical picture in which the plasma constituents are viewed as atoms, molecules, ions, and free electrons. Others have used a physical picture [9] in which all fundamental charged particles (i.e. electrons and nuclei) making up the matter under question are treated on an equal many-body footing and interactions are treated by adding two-body terms, then three-body terms and so on. This description in which complex species (atoms, ions, and molecules) arise naturally as clusters of more fundamental particles is formally exact. However, this procedure rapidly leads to very complicated many-body expressions when atoms with many electrons are involved. Our choice of the chemical picture is largely due to its theoretical transparency and adaptability to the large range of physical conditions required in opacity calculations.

HELMHOLTZ FREE ENERGY CONTRIBUTIONS

The Helmholtz free energy F is related to the canonical partition function Z of the system by the standard relation,

$$F = -kT\ln Z. \tag{1}$$

The chemical picture is closely related to the assumption of factorizability of the partition function, which allows us to write the total free energy as a sum of several contributions [1, 10],

$$F = F_1 + F_2 + F_3 + F_4 + F_5. \tag{2}$$

F_1 represents the classical ideal (Boltzmann) gas of atoms, ions, and molecules,

$$F_1 = kT\sum_{s\neq e} N_s \left[\ln\left(\frac{N_s\Lambda_s^3}{Vg_s}\right) - 1\right], \tag{3}$$

where N_s is the number of particles of species s (not including electrons), g_s is the nuclear spin statistical weight, and $\Lambda_s \equiv \sqrt{2\pi\hbar^2/m_s kT}$ is the thermal wavelength.

F_2 is the contribution related to the internal structure of species with bound electrons,

$$F_2 = \sum_{s\neq e} N_s\left(E_{s1} - kT\ln\widetilde{Z}_s\right), \tag{4}$$

where E_{s1} is the ground-state energy and $\widetilde{Z}_s$ is the effective partition function,

$$\widetilde{Z}_s \equiv \sum_j w_{sj} g_{sj} \exp\left(-\frac{E_{sj} - E_{s1}}{kT}\right). \tag{5}$$

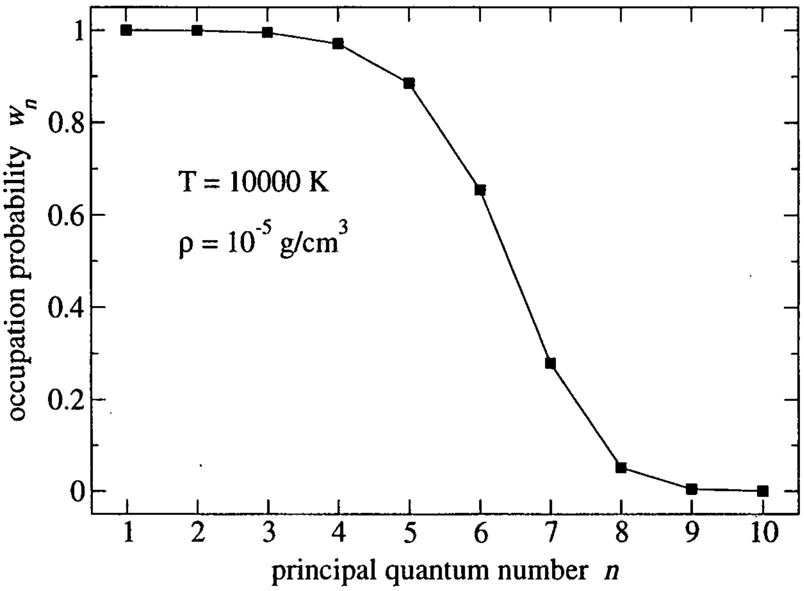

FIGURE 1. Occupation probabilities in atomic hydrogen vs. principal quantum number

The convergence of partition functions is ensured through the occupation probabilities w_{sj} that smoothly truncate the summation (see Fig. 1) by progressively reducing the effective statistical weights of excited states; they are given by,

$$w_{sj} = w_{sj}^{HS} Q_s(\beta_{sj}), \tag{6}$$

where w_{sj}^{HS} is a first-order hard-sphere contribution based on the size of the bound state [1], which is important in cold neutral systems. $Q_s(\beta)$ is the cumulative microfield distribution function and β_{sj} is the critical microfield adopted from Ref. [2] to model the destruction of bound states by the charged plasma environment.

Due to their small mass the electrons begin to display quantum degeneracy effects at much lower densities than the ions. Therefore the ideal electron gas free energy contribution is not included in F_1 but instead it is treated separately in F_3 as an ideal Fermi gas,

$$F_3 = kTN_e \left(\eta - \frac{I_{3/2}(\eta)}{I_{1/2}(\eta)} \right), \tag{7}$$

where the ideal electron chemical potential $\mu \equiv kT\eta$ is given by the implicit equation,

$$I_{1/2}(\eta) = \frac{N_e \Lambda_e^3}{2V}, \tag{8}$$

and $I_\nu(\eta) \equiv \Gamma^{-1}(\nu+1)\int_0^\infty t^\nu(\exp(t-\eta)+1)^{-1}dt$ is the non-relativistic Fermi integral.

Under low-coupling (i.e. high-temperature, low-density) conditions the Coulomb interaction term F_4 can be modeled by the well-known Debye-Hückel expression or its modification [10]. In order to cover a wide range of plasma conditions including the strongly-coupled regime we adopt the analytic fits from Refs. [5, 6, 7]. These fits take into account Monte Carlo and hypernetted-chain simulations and reproduce the proper limits (i.e. Debye-Hückel at low and Thomas-Fermi at high coupling, respectively). The excess Coulomb free energy is treated within the linear screening theory in which the ion-electron interaction is weak compared to the kinetic energy of the electrons. Then F_4 can be broken into three contributions [5],

$$F_4 = F_{ee} + F_{ii} + F_{ie}. \tag{9}$$

The ion-ion (*ii*) part is calculated from a one-component plasma model via an interpolation between Monte Carlo results for $\Gamma_i \geq 1$ and the Debye-Hückel limit and Abe correction for low-coupling conditions. The exchange-correlation (*ee*) contribution in the electron fluid comes from fits to hypernetted-chain and Monte Carlo simulations of electron one-component plasma from Ref. [7]. The electron screening (*ie*) contribution is extracted as a difference between two hypernetted-chain simulations: one for the screened and the other for the Coulomb potential.

At very low temperatures the system remains neutral across the full density range and therefore microfields $Q(\beta)$ (see Eqs. 5 and 6) cannot provide the desired effect of removing atomic bound states at high density. In order to address this problem Refs. [1, 10] introduced a pressure ionization term F_5 for neutral plasma species. Theirs was second-order in packing fraction and was based on the expansion of the low-density free energy of a system of hard spheres with an additional adjustable parameter. Since we are interested in modeling this effect at arbitrary densities, we find it more plausible to adopt the all-order free energy expression of Mansoori *et al.* [11], which is the multi-component generalization of the Carnahan-Starling formula [12]. Here we use ground-state diameters only, since at low temperatures excited states harbor negligible populations.

As was pointed out by Hummer and Mihalas [1], maintaining the thermodynamic consistency of a free-energy model with non-ideal contributions results in additional terms in the total free energy. If a non-ideal effect contributes the free energy f, then it implies an occupation probability w_{sj} in the effective partition functions,

$$w_{sj} = \exp\left(-\frac{1}{kT}\frac{\partial f}{\partial N_{sj}}\right) \tag{10}$$

and a self-consistency term in the free energy,

$$-\sum_{sj} N_{sj}\frac{\partial f}{\partial N_{sj}}, \quad \text{or,} \quad kT\sum_{sj} N_{sj}\ln w_{sj}, \tag{11}$$

where N_{sj} is the population of the ground or excited state j in the species s. Therefore in principle non-ideal effects enter the model in three places. In our model the plasma non-ideality is accounted for in terms F_2, F_4, and F_5. In F_2 the occupation probabilities

(Eq. 6) were constructed in such a way that the corresponding non-ideal free energy contribution f is linear in populations N_{sj} and hence it will be canceled by its associated self-consistency term from Eq. 11. Furthermore, the Coulomb and pressure-ionization terms (F_4 and F_5) only depend on total species populations $N_s \equiv \sum_j N_{sj}$; therefore the associated occupation probabilities (Eq. 10) will factor out of the partition functions $\widetilde{Z}_s$ in F_2 (Eq. 4) and cancel with the accompanying self-consistency term (Eq. 11). Thus the surviving non-ideal terms $f = F_4 + F_5$, together with occupation probabilities w_{sj} in F_2, provide a full and consistent account of all non-ideal effects included in our model.

FREE-ENERGY MINIMIZATION

The minimization procedure consists of finding the particular set of populations $\{N_s\}_{min}$ that minimizes the expression for $F(V,T,\{N_s\})$ while holding volume and temperature constant. This is equivalent of finding the state of maximum entropy and describes the system at thermodynamic equilibrium.

The populations $\{N_s\}$ must satisfy several conditions: stoichiometric constraints, overall charge neutrality of the plasma, and total mass conservation. For ionization-recombination reactions $A^{i+} \rightleftharpoons A^{(i+1)+} + e^-$ the free-energy minimization requires,

$$\left(\frac{\partial F}{\partial N_i}\right)_{T,V,\{N_{j\neq i}\}} = \left(\frac{\partial F}{\partial N_{i+1}}\right)_{T,V,\{N_{j\neq i+1}\}} + \left(\frac{\partial F}{\partial N_e}\right)_{T,V,\{N_{j\neq e}\}}. \tag{12}$$

This can be equivalently written in terms of the chemical potentials as $\mu_i = \mu_{i+1} + \mu_e$. If there are N ion stages involved then there will be $N-1$ coupled ion population equations of this form. The system of equations is then closed by the conservation equations,

$$N_e = \sum_{s\neq e} z_s N_s, \tag{13}$$

$$m_{tot} = \sum_{s\neq e} m_s N_s, \tag{14}$$

where z_s is the charge of species s in units of elementary charge e. (These equations can also be modified to describe molecular dissociation.) Given our adopted free-energy model, Eq. 12 becomes,

$$\frac{N_{i+1}}{N_i} = \frac{\widetilde{Z}_{i+1}}{\widetilde{Z}_i} \exp\left[-\left(\chi_i - \phi_i + \mu\right)/kT\right], \tag{15}$$

in which $\chi_i \equiv E_{i+1,1} - E_{i1}$ is the unperturbed ionization potential and μ is the ideal electron chemical potential given by Eq. 8. Eq. 15 formally resembles the traditional Saha equation with the additional term ϕ_i, which is given by,

$$\phi_i = \left(\frac{\partial F_4}{\partial N_i}\right) - \left(\frac{\partial F_4}{\partial N_{i+1}}\right) - \left(\frac{\partial F_4}{\partial N_e}\right) + \left(\frac{\partial F_5}{\partial N_i}\right) - \left(\frac{\partial F_5}{\partial N_{i+1}}\right) + \\ + kT \sum_{s \neq e} \frac{N_s}{\tilde{Z}_s} \left[\left(\frac{\partial \tilde{Z}_s}{\partial N_{i+1}}\right) + \left(\frac{\partial \tilde{Z}_s}{\partial N_e}\right) - \left(\frac{\partial \tilde{Z}_s}{\partial N_i}\right) \right] . \tag{16}$$

This term ϕ_i enters the modified Saha Eq. 15 subtracted from the unperturbed ionization potential χ_i and thus could in principle be interpreted as the contribution due to "continuum lowering." In fact, other models [13] treat non-ideal plasma effects solely by reducing the ionization potential in the Saha equation without regard to thermodynamic consistency. We emphasize that our model is not a "continuum-lowering" model in this sense. Since ϕ_i (like everything else in our model) is derived from the Helmholtz free energy, it models non-ideal plasma effects in a thermodynamically consistent way by incorporating corrections to species' chemical potentials arising from interactions in the plasma. In addition, in our model bound states are removed not only by an effective change of ionization potentials but also by reduction of their effective statistical weights by the occupation probabilities in the partition functions (Eqs. 5 and 6).

An alternative method of minimizing F is to simply scan the free energy surface for a global minimum. In either method care must be taken to avoid a possible local minimum of the free energy which will not represent the $\{N_s\}_{min}$ corresponding to true thermodynamic equilibrium.

While the free-energy-surface scan is the simplest way of finding $\{N_s\}_{min}$, its computational cost scales very poorly with the number of species in the model. Some improvement can be obtained by using a successive refinement procedure in which the free-energy surface is scanned several times on a progressively finer mesh. Yet another approach would be to use a genetic algorithm search technique [14] in which the fitness function (to be maximized) is chosen as the negative of the free energy. Genetic algorithms work very well and fast in complex and multidimensional parameter spaces, they are rather immune against getting stuck in local minima, and they do not require user-supplied derivatives of the fitness function. We have successfully tested a particular implementation of a genetic algorithm [15] in the simple case of hydrogen plasma as a proof of principle. In general cases one could use a combination of techniques: a genetic algorithm to quickly locate the general vicinity of the free-energy minimum (in which the free energy surface is more likely to have a "regular" behavior) and then use a deterministic method such as Eqs. 13,14,15 to refine the solution $\{N_s\}_{min}$ to the desired accuracy.

Once the free energy has been minimized, all further thermodynamic quantities can also then be obtained from the expression for the free energy using the set of populations $\{N_s\}_{min}$ and standard thermodynamic formulae. For example, pressure P and internal energy E are given by,

$$P = -\left(\frac{\partial F}{\partial V}\right)_{T,\{N_j\}}, \quad \text{and,} \quad E = -T^2 \left(\frac{\partial (F/T)}{\partial T}\right)_{V,\{N_j\}} . \tag{17}$$

We can then go on to obtain all other thermodynamic quantities (such as compressibilities, specific heats, etc.) in a similar manner. Since these are all derivable ultimately from the free energy F and the set $\{N_s\}_{min}$, thermodynamic consistency (fulfillment of the Maxwell relations) is ensured. Additionally, since our approximation for the free energy is analytic, we can calculate these thermodynamic quantities analytically and avoid the risk of sometimes inaccurate numerical differentiation.

Finally, for line spectrum calculations, excited state populations N_{sj} can be extracted from the total populations per ion stage $\{N_s\}_{min}$ via a modified Boltzmann relation [1],

$$N_{sj} = \frac{N_s}{\tilde{Z}_s} w_{sj} g_{sj} \exp\left(-\frac{E_{sj} - E_{s1}}{kT}\right). \tag{18}$$

Occupation probabilities w_{sj} can also be used to model the smooth merging of a Rydberg line series with its corresponding bound-free edge [4, 16].

RESULTS

As a first step we applied our model to hydrogen plasma in which we test the interplay of all the various free-energy contributions. We include ionized (H^+), atomic (H), negative ion (H^-), neutral molecular (H_2), and ionized molecular (H_2^+) hydrogen in our model. The description of electronic, vibrational, and rotational states of the H_2 and H_2^+ molecules is adopted from Refs. [17, 18].

In Fig. 2 we compare our results for the pressure with path-integral Monte Carlo (PIMC) calculations [19] and in Fig. 3 with quantum molecular dynamics (QMD) [20]. A very good agreement between our chemical model and the two *ab initio* calculations is shown in both cases. This level of agreement was not possible with an earlier version of our model which implemented the Coulomb (F_4) and hard-sphere pressure-ionization (F_5) terms according to [10]. In this older model that used a τ-modified Debye-Hückel (DH) formula for F_4 and a second-order expression for F_5 the calculated pressures were too high by up to an order of magnitude vs. PIMC and QMD. In the strongly-coupled regime the absolute values of the DH free energy are too large, while in its τ-modified version they are too low. Our adopted fits for F_4 [5, 6, 7] follow the DH results at low-coupling and then go between the DH and τ-modified DH values, as expected.

The second-order expression for the hard-sphere term F_5 from [10] was seen to provide a pressure-ionization effect that removes bound species too rapidly at densities that are too low. This results from the definition of the packing fraction used in [10] that is larger than the usual expression by the factor of 8. In this previous model an additional adjustable parameter was used in F_5 to further increase the pressure-ionization effect. Our current model already produced a fair agreement with the pressure data from PIMC and QMD without any additional *ad hoc* parameters; the degree of agreement was further improved by allowing the original hard-sphere radii used for H (5.3×10^{-9} cm, i.e. the Bohr radius) and H_2 (9.0×10^{-9} cm) to be reduced by (at this point) an *ad hoc* factor. For the comparison with PIMC (Fig. 2) this factor is 0.6 and for QMD (Fig. 3) it is 0.5. This is consistent with the finding [21] that effective hard-sphere radii can be used to represent the softness of the repulsive parts of interparticle potentials.

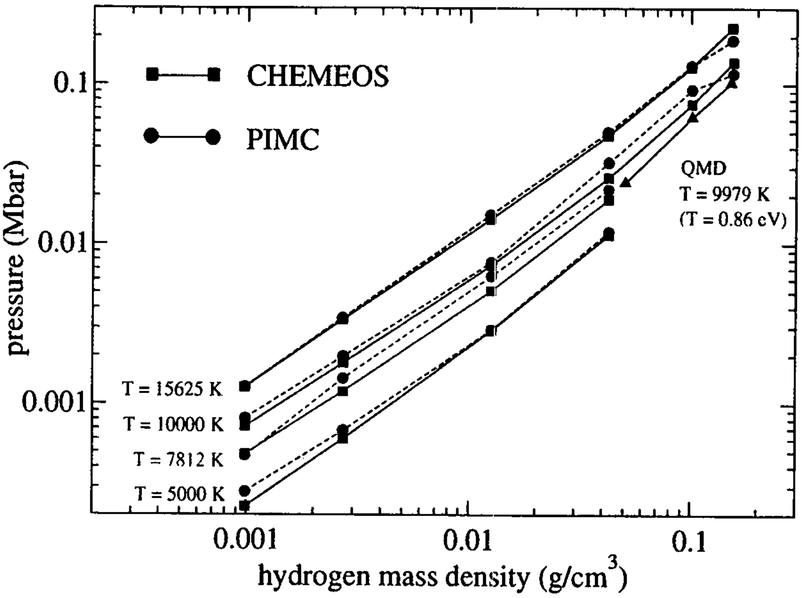

FIGURE 2. Comparison of CHEMEOS and path-integral Monte Carlo pressures

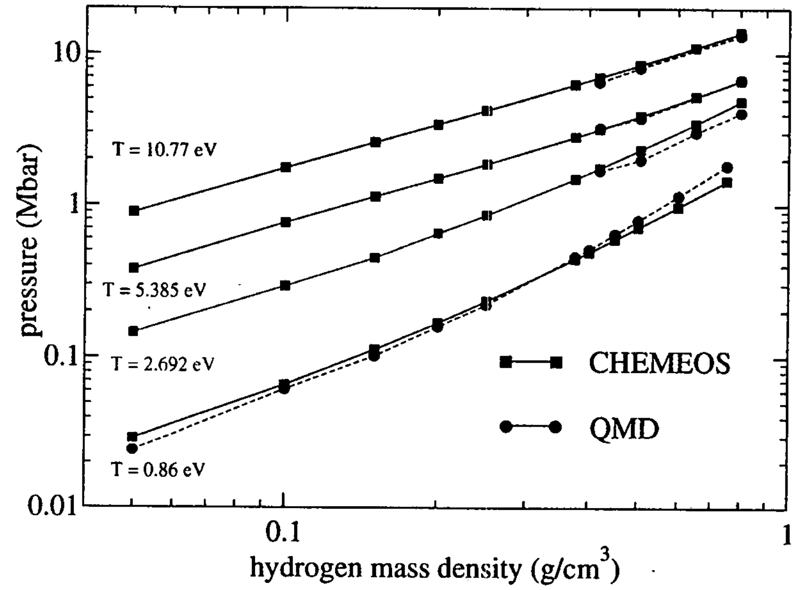

FIGURE 3. Comparison of CHEMEOS and quantum molecular dynamics pressures

The comparison of internal energies (Eq. 17) with PIMC in the 10^{-3}-$10^{-1} g/cm^3$ density range shows excellent agreement for the four highest temperatures as well as for the lowest temperature (5000 K). In the high-temperature cases the plasma is nearly completely ionized, whereas at 5000 K the system is nearly 100% molecular hydrogen. Certain disagreement exists at 7812, 10000, and 15625 K, where the system is still neutral but is partially dissociated. Similar disagreements between CHEMEOS and PIMC also appear in the estimates of H and H_2 populations. This suggests the need for an improved treatment of neutral-neutral interactions in our model, possibly by going beyond the simple hard-sphere description. This could be accomplished by the use of actual interparticle potentials that model the soft-core repulsion and even a weak van-der-Waals attraction. Such features should improve the accuracy of the $H_2 \rightleftharpoons 2H$ dissociation-recombination equilibrium and hence internal energy comparisons with *ab initio* calculations. These enhancements could also possibly address the problems caused by the relative flatness and possible "roughness" of the free-energy landscape around its global minimum. We have seen indications in our current model that this indeed is an issue, because of which the populations can change discontinuously with a minute change of input conditions (temperature or density) or a small change in the physics of the model (such as the choice of effective hard-sphere diameters). These problems may also be artifacts of the above mentioned inadequate neutral-neutral treatment, and therefore could be addressed by the same improvements.

Another aspect of our model that requires further attention is the observed "plateau" in the degree of ionization as the densities approach conditions in which no atoms can exist by simple geometric arguments. The responsibility for the appearance of this behavior can be traced to the degeneracy of the free electrons (term F_3, Eq. 7) which discourages further pressure ionization, while the destruction of bound states by plasma microfields (term F_2, Eqs. 4 and 6) is not sufficiently competitive in our present model. The microfields we are currently using do not account for the reduction of electron screening due to degeneracy. The use of microfields that take this effect into account would lead to larger microfield values experienced by species with bound electrons. This would cause a stronger destruction of bound states, which should result in a smooth transition from the partially to the fully pressure-ionized plasma state.

CONCLUSIONS AND FUTURE WORK

We presented first results of a new equation-of-state model CHEMEOS currently under development at the Los Alamos National Laboratory. The model is based on the chemical-picture approach combined with an occupation-probability formalism. The choice of this technique was motivated by the ultimate purpose of this model, which is its incorporation into a new Los Alamos opacity code ATOMIC. Chemical models have long been recognized as a convenient and computationally efficient means for EOS calculations. As a first test, we applied our model to the "simplest" case of hydrogen, in which the number of species is limited and independent calculations using other theories are available. Such comparisons with path-integral Monte Carlo and quantum molecular dynamics calculations are particularly important in high-density regimes where the basic assumptions behind the chemical picture break down. Preliminary comparisons of calculated pressures are encouraging, especially in the light of substantial disagreements of PIMC and QMD with the previous version of the CHEMEOS model. These discrepancies have now been addressed by a more accurate treatment of the Coulomb and hard-sphere pressure-ionization contributions to the free energy. Further possible improvements include a more rigorous description of the softness of the repulsive part of interparticle potentials and more accurate microfield distributions with reduced screening due to electron degneracy. Ultimately we also plan to cross-check our hydrogen results with experimental and astrophysical data, and then implement the model for treatment of any low-to-medium Z treatment within ATOMIC.

ACKNOWLEDGMENTS

This work has been performed under the auspices of the U.S. Department of Energy and the University of California.

REFERENCES

1. Hummer, D., and Mihalas, D., *Ap.J.*, **331**, 794 (1988).
2. A. Nayfonov, *et al.*, *Ap.J.*, **526**, 451 (1999).
3. H.C. Graboske Jr., *et al.*, *Phys. Rev. A*, **3**, 1419 (1971).
4. I. Hubeny, *et al.*, *Astron. Astrophys.*, **282**, 151 (1994).
5. Chabrier, G., and Potekhin, A., *Phys. Rev. E*, **58**, 4941 (1998).
6. Potekhin, A., and Chabrier, G., *Phys. Rev. E*, **62**, 8554 (2000).
7. S. Ichimaru, *et al.*, *Phys. Rep.*, **149**, 91 (1987).
8. Däppen, W., *Astron. Astrophys.*, **91**, 212 (1980).
9. F. J. Rogers, *et al.*, *Astroph. J.*, **456**, 902 (1996).
10. D. Mihalas, *et al.*, *Ap.J.*, **331**, 815 (1988).
11. G.A. Mansoori, *et al.*, *J. Chem. Phys.*, **54**, 1523 (1971).
12. Carnahan, N., and Starling, K., *J. Chem. Phys.*, **51**, 635 (1969).
13. N.H. Magee, *et al.*, in *Astrophysical Applications of Powerful New Databases*, edited by S. J. Adelman and W. Wiese, Astronomical Society of the Pacific, San Francisco, 1995, p. 51.
14. Goldberg, D. E., *Genetic Algorithms in Search, Optimization, and Machine Learning*, Addison-Wesley, 1989, ISBN 0-201-15767-5.
15. Louis, S. J., `http://www.cs.unr.edu/~sushil/`.
16. W. Däppen, *et al.*, *Ap.J.*, **319**, 195 (1987).
17. Saumon, D., and Chabrier, G., *Phys. Rev. A*, **44**, 5122 (1991).
18. Huber, K., and Herzberg, G., *Molecular Spectra and Molecular Structure. IV Constants of diatomic molecules*, Van Nostrand Reinhold, 1979, ISBN 0-442-23394-9.
19. Militzer, B., and Ceperley, D., *Phys. Rev. E*, **63**, 066404 (2001).
20. S. Mazevet, *et al.*, *Astron. Astrophys.*, **405**, L5 (2003).
21. J. Weeks, *et al.*, *J. Chem. Phys.*, **54**, 5237 (1971).

This research is supported by the Department of Energy under contract W-7405-ENG-36.